AIMS Materials Science, 3(1): 270-288.
DOI: 10.3934/matersci.2016.1.270
Received: 15 January 2016
Accepted: 28 February 2016
Published: 02 March 2016

http://www.aimspress.com/journal/Materials

Short review

Photoactivated Fuel Cells (PhotoFuelCells). An alternative source of renewable energy with environmental benefits

Stavroula Sfaelou and Panagiotis Lianos *

Department of Chemical Engineering, University of Patras, 26500 Patras, Greece

* **Correspondence**: Email: lianos@upatras.gr.

Abstract: This work is a short review of Photoactivated Fuel Cells, that is, photoelectrochemical cells which consume an organic or inorganic fuel to produce renewable electricity or hydrogen. The work presents the basic features of photoactivated fuel cells, their modes of operation, the materials, which are frequently used for their construction and some ideas of cell design both for electricity and solar hydrogen production. Water splitting is treated as a special case of photoactivated fuel cell operation.

Keywords: Photoactivated Fuel Cells; photocatalytic fuel cells; PhotoFuelCells; solar cells; hydrogen production

1. Introduction

Solar energy can be converted into electricity or chemical energy by various techniques, photovoltaics being the most direct. Large scale production of electricity by solar energy conversion should, however, be supported by procedures of energy storage. One way to store energy is to convert it into chemical energy, in particular, hydrogen. In this respect, photoelectrochemical conversion of solar energy provides the most promising routes for this purpose and for this reason it has become one of the most studied scientific domains of the recent years. The origins of the photoelectrochemical cells date back to the work of Alexander-Edmond Becquerel in 1839 [1] but it is the work of Fujishima and Honda, more than 40 years ago [2], that has set the basis of modern

photoelectrochemistry and has created one of the most popular research fields with ever growing number of adepts.

Photoactivated Fuel Cells (also named Photocatalytic Fuel Cells or PhotoFuelCells, PFCs) [3–10] constitute an interesting domain in the study of photoelectrochemical cells. PFCs photoelectrocatalytically oxidize a fuel to produce electricity or storable chemical energy, mainly hydrogen. As any standard photoelectrochemical cell, PFCs comprise a photoanode electrode carrying a photocatalyst, a cathode (counter) electrode carrying a reduction electrocatalyst and an electrolyte. The photocatalyst is in the form of mesoporous nanocrystalline semiconductor film. Large band gap semiconductors like nanocrystalline titania (nc-TiO_2) may be combined with a sensitizer, which is also a nanoparticulate semiconductor of lower band gap absorbing visible light [11]. The second major component, the electrocatalyst, is usually made of a dispersion of Pt nanoparticles in nanoparticulate carbon [12] while the electrolyte is an aqueous solution of either a neutral salt, or an acid or a base, depending on the desired in each case pH value. Figure 1 illustrates two examples of PFC cells, one used for production of electricity and the second for production of hydrogen. Photons are absorbed by the photoanode generating electrons and holes. Electrons flow through an external circuit and they are led to the counter electrode where they participate in reduction reactions. Holes oxidize the fuel at the photoanode. Thus both photogenerated electrons and holes are consumed in chemical reactions and they do not recombine in a cyclic manner as it happens in photovoltaic cells. A PFC may be configured in 1 or 2 compartments as those illustrated in Figure 1, depending on the particular application. More on this matter will be discussed in the following sections.

The fuel which is used to feed a PFC, may be an organic or an inorganic substance and it is dissolved in the electrolyte of the anode compartment. The fuel is photocatalytically degraded and consumed at the photoanode producing electricity or chemical energy, hence the name (Photoactivated) Fuel Cell. Photocatalytic oxidation can be carried out with many organic or inorganic substances including water itself. Photocatalytic oxidation functions not only with pure chemical substances but also with their mixtures, therefore, materials, which are considered water soluble wastes or pollutants may be used as fuel in PFCs, thus offering the double environmental benefit of renewable energy production with environmental remediation by consumption of wastes. Most efficient organic fuels are those of $C_xH_yO_z$ composition, i.e. alcohols, diols, organic acids and carbohydrates, which may be products of biomass. Therefore, a large family of fuels may derive from biomass products [13], which, for example, are too costly to process by other methods and they could be used as fuel in PFCs. Photoactivated Fuel Cells then constitute an important alternative technology for renewable energy production.

2. Description of Standard Modes of PFC Operation

A PFC may be operated in two main operation modes, either to produce electricity or to produce hydrogen. In both cases, photons are absorbed by the photoanode generating electron-hole pairs. Depending on the nature and the quality of the photocatalyst, a substantial percentage of these charge carriers recombine and their energy is dissipated. Those escaping recombination take active part in oxidation and reduction reactions. Most electrons are channeled through an external circuit to the

counter electrode where they take part in reduction reactions, which are represented in Table 1 by reactions (V-VIII). In the absence of oxygen, they produce molecular hydrogen either by reduction

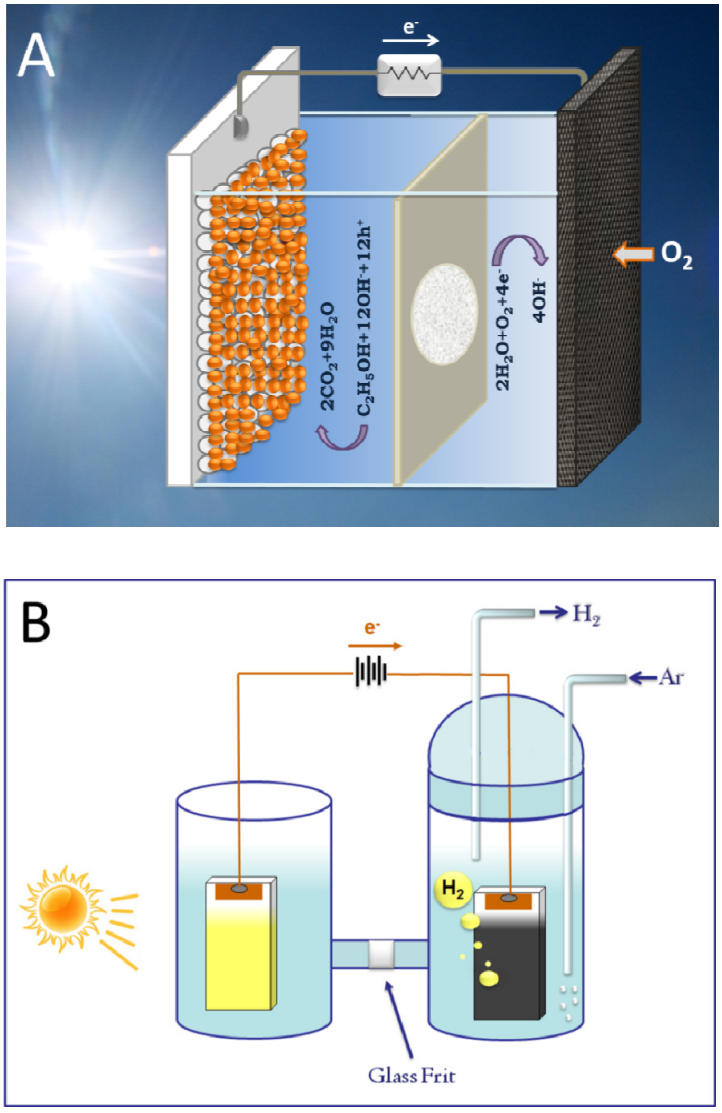

Figure 1. Schematic illustration of two PFC cells: (A) for electricity and (B) for hydrogen production. In cell A, the photoanode also plays the role of reactor window. The counter electrode (cathode) is made of a porous material allowing diffusion of atmospheric oxygen. A diaphragm bearing an ion transfer membrane separates the cell into two compartments. In cell B, hydrogen is produced under electric forward bias and is monitored using Ar as inert carrier gas. A glass frit is used as ion-transfer membrane.

of protons or by reduction of water. Depending on the pH and the availability of protons, one or the other reaction may prevail or they may both take place simultaneously. At high pH, protons cannot survive since they interact with OH^- producing water. Therefore in that case molecular hydrogen is generated by reduction of water. The redox potential at which reduction takes place depends on the pH according to the following standard rule:

$$\Delta V(Volts) = -0.059 \times \Delta pH \quad (1)$$

where ΔV is the variation of the value of the potential that corresponds to a variation of the pH equal to ΔpH. Thus when the pH is very low (acidic pH) the potential is close to 0.0 V *vs* NHE. At pH = 13 (alkaline pH), as shown in Table 1, the potential is −0.77 V *vs* NHE. In the presence of oxygen, the latter takes part in reduction reactions, both at low and high pH. The potential at which reaction is carried out varies then between +1.23 to +0.46 V *vs* NHE. The potential is obviously defined in that case by the following rule:

$$V(Volts) = +1.23 - 0.059 \times pH \quad \text{(presence of } O_2\text{)} \quad (2)$$

Table 1. Oxidation and reduction reactions taking place in a PFC employing ethanol as model fuel.

<table>
<tr><td colspan="2">Photoanode</td></tr>
<tr><td colspan="2">Photons are absorbed by a semiconductor photocatalyst SP either directly or by means of a sensitizer
$SP + h\nu \rightarrow e^- + h^+$ (I)
Most photogenerated electrons, which escape recombination, flow in the external circuit. Some may interact with O_2, if present, producing superoxide and finally hydroxyl radicals. Photogenerated holes, which avoid recombination, interact with the fuel by the following principal reaction schemes:
$C_2H_5OH + 3H_2O + 12h^+ \rightarrow 2CO_2 + 12H^+$ (low pH) (II)
$OH^- + h^+ \rightarrow OH^\bullet$ and $C_2H_5OH + 12OH^\bullet \rightarrow 2CO_2 + 9H_2O$ (high pH) (III)
Intermediate steps may involve interaction of the fuel with photogenerated holes in the valence band of the semiconductor photocatalyst or in the combined oxidation level of the semiconductor-sensitizer combined photocatalyst while one-hole interactions are also possible and they are particularly interesting since they are at the origin of the current doubling effect.
$C_2H_5OH + 2h^+ \rightarrow CH_3CHO + 2H^+$ (IVa)
$C_2H_5OH + h^+ \rightarrow C_2H_5O^\bullet + H^+$ (IVb)
$C_2H_5OH + OH^\bullet \rightarrow C_2H_5O^\bullet + H_2O$ (IVc)</td></tr>
<tr><td colspan="2">Cathode</td></tr>
<tr><td>Inert environment (no O_2 present)</td><td>Aerated electrolyte or cathode exposed to ambient air</td></tr>
<tr><td>• Low pH (potential: 0.00 V at pH = 0)
$2H^+ + 2e^- \rightarrow H_2$ (V)
• Alkaline pH (potential: −0.77 V at pH = 13)
$2H_2O + 2e^- \rightarrow H_2 + 2OH^-$ (VI)</td><td>• Low pH (potential: 1.23 V at pH = 0)
$2H^+ + ½\ O_2 + 2e^- \rightarrow H_2O$ (VII)
• Alkaline pH (potential: 0.46 V at pH = 13)
$H_2O + ½\ O_2 + 2e^- \rightarrow 2OH^-$ (VIII)</td></tr>
<tr><td colspan="2">Overall cell reactions (combination of anode and cathode reactions)</td></tr>
<tr><td colspan="2">• absence of oxygen (ethanol reforming): $C_2H_5OH + 3H_2O \rightarrow 2CO_2 + 6H_2$ (IX)
• presence of oxygen (ethanol mineralization): $C_2H_5OH + 3O_2 \rightarrow 2CO_2 + 3H_2O$ (X)</td></tr>
</table>

Reduction reactions do not take place automatically since they necessitate the presence of an electrocatalyst, which reduces the over-potential established between the electrode and the liquid

electrolyte phase. The electrocatalyst is in the form of a thin mesoporous film and its standard composition, as already said, is carbon nanoparticles mixed with Pt nanoparticles [12]. Because Pt is rare and expensive, an intense effort is made in the search for alternative materials [14–18]. Some examples will be presented also in the present work. Since the role of the electrocatalyst is to facilitate electron exchange with the liquid electrolyte phase, thus eliminating over-potential, the operation potential of the counter electrode may be considered to be the same as the electrochemical potential of the corresponding reduction reactions.

Holes participate in oxidation reactions, which, of course, take place at the photoanode. When the sacrificial agent is attached on the surface of the photocatalyst, it is possible to donate an electron and thus eliminate hole. However, experience shows that in most of the cases involving organic sacrificial agents, oxidation is done in solution by the intermediate of hydroxyl radicals $^{\bullet}OH$. Hydroxyl radicals are created by interaction of hydroxyl ions with holes:

$$OH^- + h^- \rightarrow {}^{\bullet}OH \tag{3}$$

The electrochemical potential of hole scavenging by OH^- is 2.02 *vs* NHE (at pH zero) and, of course, varies with pH according to Eq.(1). It is concluded that the oxidation level of the semiconductor photocatalyst or the combined photocatalyst/co-catalyst(sensitizer) must be more positive than the $^{\bullet}OH/OH^-$ level in order to generate hydroxyl radicals and oxidize organic fuel. Several metal oxide semiconductors have this capacity but several others have not. Figure 2 presents a diagram of a few selected semiconductor photocatalysts and a few characteristic redox potentials. The oxidation level of a semiconductor is its valence band (VB) level where the photogenerated holes reside. It is seen that most semiconductors illustrated in Figure 2 can produce hydroxyl radicals. When, however, a semiconductor photocatalyst is combined with a sensitizer, holes may be injected into the valence band of the sensitizer and in that case their oxidation level may decrease, as illustrated in Figure 3. It is then possible, as it will be further discussed later, that the combined photocatalyst may lose its capacity to generate hydroxyl radicals [11]. Other oxidation reactions are carried out at lower potentials, for example in the case of sulfide/sulfite electrolytes, which are frequently employed for hydrogen production [18]. The corresponding redox potentials for two characteristic oxidation reactions are the following [19]:

$$2SO_3^{2-} + 2h^+ \rightarrow S_2O_6^{2-} \qquad (-0.25 \text{ V } \textit{vs} \text{ NHE at pH 14}) \tag{4}$$

$$2S^{2-} + 2h^+ \rightarrow S_2^{2-} \qquad (-0.52 \text{ V } \textit{vs} \text{ NHE at pH 14}) \tag{5}$$

These values correspond to +0.58 and +0.31 V at pH zero. All semiconductors illustrated in Figure 2 are then capable of oxidizing sulfide and sulfite species.

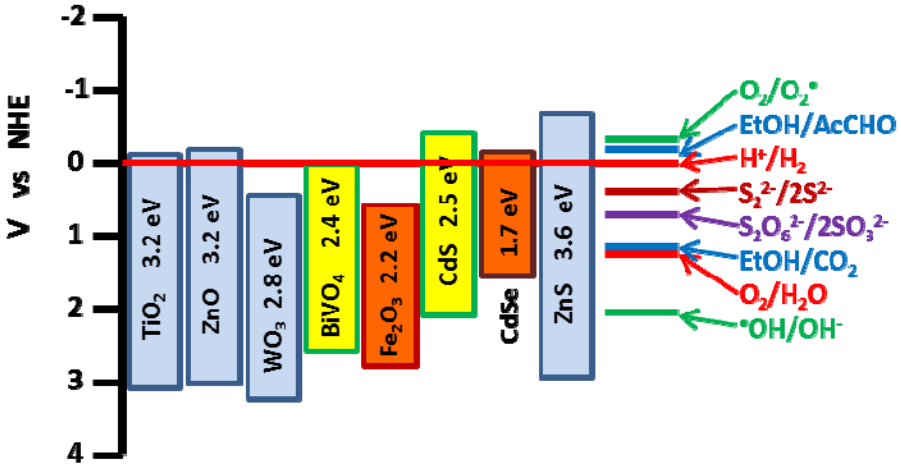

Figure 2. Energy levels for a few selected semiconductor photocatalysts and a few redox levels of selected reactions. All values correspond to pH zero.

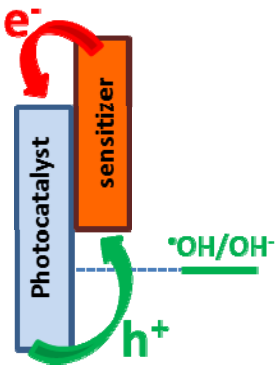

Figure 3. Illustration of the process of sensitization and hole transfer in combined semiconductor photocatalysts.

Water itself can be also oxidized by several semiconductor photocatalysts. The water oxidation level, as it is well known, lies at 1.23 V *vs* NHE at pH zero. Pure water oxidation leads to generation of molecular oxygen, however, oxygen emission is hardly detected in the presence of sacrificial agents. In addition, a matter that is rather neglected, peroxide species may be encouraged [20] instead of molecular oxygen production.

Figure 2 also depicts oxidation levels E^0 of ethanol. These values were calculated by the following standard formula:

$$E^0 = \frac{\Delta G^0}{-nF} \tag{6}$$

where n is the number of electron moles involved in the oxidation reaction and F is the Faraday constant 96.486 kC mol^{-1}, while ΔG^0 is given in kJ mol^{-1}. A few selected ΔG^0 values are listed in Table 2 and the corresponding values of n and E^0 are listed in Table 3. The number of electrons (and holes) is equal to the number of holes involved in reactions (II-IV) of Table 1. In reality, oxidation of ethanol proceeds by intermediate steps the first of which is the formation of acetaldehyde [21]. CH_3CHO/CH_3CH_2OH oxidation level is negative, as seen in Table 3. Therefore, any of the illustrated in Figure 2 semiconductors can in principle oxidize ethanol. This is, however, not what is obtained in practice [11,22] and thus it is concluded, as will be discussed later, that oxidation of ethanol mainly proceeds by hydroxyl radicals. The same is true for all organic substances.

Table 2. Standard molar Gibbs free energy change of formation at 25 ^oC for a few selected chemical substances.

Compound	**ΔG^0(kJ mol^{-1})**
water	−237.14
carbon dioxide (gas)	−394.4
ethanol	−174.8
acetaldehyde	−134.0

Table 3. Calculated Gibbs free energy change and standard potential for ethanol oxidation reactions.

Ethanol oxidation reaction	**Number of charges**	**ΔG^0(kJ mol^{-1})**	**E^0 (V)**
$C_2H_5OH \rightarrow CH_3CHO+H_2$	2	+40.8	−0.21
$C_2H_5OH + 3O_2 \rightarrow 2CO_2 + 3H_2O$	12	−1325.4	+1.14
$C_2H_5OH + 3H_2O \rightarrow 2CO_2 + 6H_2$	12	+97.4	−0.08

The final products of the oxidation reactions at the photoanode electrode depend on solution pH and on the presence or absence of O_2. In the absence of O_2 and at low pH, holes mediate the generation of hydrogen ions H^+ according to reaction (II) of Table 1. Reaction (II) represents an overall scheme. In reality, reaction proceeds by steps, where the following route usually prevails [4,21]:

$$\text{ethanol} \rightarrow \text{acetaldehyde} \rightarrow \text{acetic acid} \rightarrow CO_2+H_2O \quad (7)$$

Most of these intermediate reactions are endothermic. The Gibbs free energy change for reaction (II) of Table 1 is positive, therefore the overall balance is endergonic and is mediated by photogenerated holes. The same holds true for all reactions associated with chemical substances of the general composition $C_xH_yO_z$, which are generalized by the following scheme [4,23,24]:

$$C_xH_yO_z + (2x-z)H_2O + (4x+y-2z)h^+ \rightarrow xCO_2 + (4x+y-2z)H^+ \quad (8)$$

At high pH, a lot of $^{\bullet}OH$ radicals are formed by interaction of OH^- with holes through reaction (3), therefore, photocatalytic degradation should be visualized with their participation. In reality, ethanol photodegradation still follows the route of Eq.(7) through intermediate acetaldehyde formation, as it has been previously detected and analyzed [25]. However, the number of hydrogen ions should be limited at high pH or completely eliminated by interacting with OH^- and producing water. Thus at high pH the photocatalytic degradation of ethanol should be more realistically represented by reaction (III) of Table 1 while a more general scheme equivalent to Eq.(8) should be defined by the following equation:

$$C_xH_yO_z + (4x + y - 2z)^{\bullet}OH \rightarrow xCO_2 + (2x + y - z)H_2O \quad (9)$$

where we assume that $H^+ + OH^- \rightarrow H_2O$ and $H_2O + h^+ \rightarrow H^+ + {}^{\bullet}OH$. In the presence of oxygen, alternative photocatalytic degradation routes may be activated, however, what is mainly affected by the presence of oxygen is the production of molecular hydrogen. We have previously found that the presence of O_2 accelerates mineralization of ethanol [25,26] at the expense of the current flowing in the external circuit. Particular attention must be paid to the one-hole interactions (IVb and IVc) of Table 1, showing ethanol radical formation. This radical is unstable and by interaction with the photocatalyst it injects an electron into its conduction band. This is responsible for the so-called "Current Doubling" effect [27,28].

When reactions (V-VIII) are combined with reactions (II and III) they yield the characteristic schemes of cell operation, which are independent of the pH but distinguish themselves by the presence or not of oxygen. Thus electric current flows through the external circuit and hydrogen is produced in the absence of oxygen while in its presence only electricity is produced. These two overall operation schemes are represented by reactions (IX) and (X) of Table 1. The corresponding schemes for substances of the general composition $C_xH_yO_z$ [5] are given by

$$C_xH_yO_z + (2x - z)H_2O \rightarrow xCO_2 + (2x + \frac{y}{2} - z)H_2 \quad (10)$$

in the absence of oxygen (photocatalytic reforming) and by

$$C_xH_yO_z + (x + \frac{y}{4} - \frac{z}{2})O_2 \rightarrow xCO_2 + \frac{y}{2}H_2O \quad (11)$$

in the presence of oxygen (photocatalytic degradation).

The driving force for PFC operation in either of the above modes is the potential difference established between the photoanode and the counter electrode. The materials of the electrodes themselves might introduce some bias but this is in practice low. As already said, the potential of the counter electrode is mainly defined by the type of the reduction scheme, which is affected by the presence or not of O_2 and by the value of the pH. On the other hand, the potential of the photoanode depends on the position of the conduction band of the semiconductor photocatalyst and on its Fermi level. For practical purposes, most researchers, use the conduction band level of n-type nanocrystalline semiconductors as a handy index of the photoanode potential. When the

semiconductor is excited, its CB level becomes more negative and when a sacrificial agent is present consuming holes and liberating more electrons, the level becomes even more negative. The open circuit voltage V_{oc} measured in a PFC reflects the potential difference between photoanode and counter electrode. Thus V_{oc} is low in the dark, becomes higher under illumination and becomes even higher in the presence of a sacrificial agent. Indeed, as seen in the example of Figure 4, showing current-voltage curves for a standard PFC functioning with aerated counter electrode and a photoanode bearing nanocrystalline titania photocatalyst (nc-TiO_2), V_{oc} was 0.35 V in the dark, 0.75 V under illumination and increased further to about 1.1 V in the presence of ethanol. These values of photovoltage are relatively high but they are justified by the following considerations. The CB of nc-TiO_2 is located approximately at −0.2 V *vs* NHE and oxygen reduction at +1.23 V *vs* NHE (values correspond to pH zero). This creates a difference of 1.43 V. Such value cannot be reached, due to inevitable losses, but justifies the actual experimental voltage measured in Figure 4. If the counter electrode is kept in an inert environment in the absence of oxygen, hydrogen is produced by reduction of protons or water at a potential equal to 0.0 V *vs* NHE (pH zero).The potential difference between photoanode and counter electrode is then too small and it does not provide enough drive to run the system. It is then necessary to apply an external bias and this has been demonstrated in several works both by us and other authors. There are some photocatalysts with high enough CB which theoretically may photoelectrocatalytically produce hydrogen without bias but in practice this is not frequently reported. On the contrary, the vast majority of works involve the application of a forward bias (*cf.* Figure 1B). A forward bias can be also of chemical nature. If the cell is composed of two compartments and the anode compartment is filled with an alkaline electrolyte while the cathode compartment contains an acidic electrolyte a chemical forward bias is applied with a theoretical value calculated according to Eq.(1).

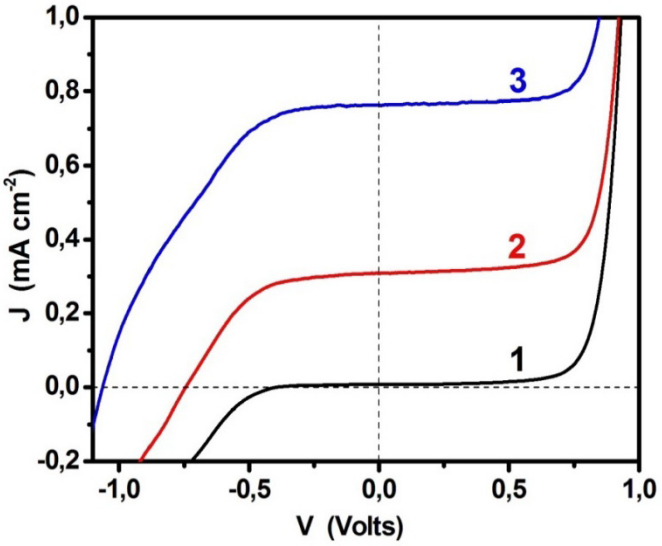

Figure 4. Current-voltage curve for a PFC operating with an aerated cathode and nc-TiO_2 photoanode: (1) dark current; (2) illuminated photoanode-no additives; and (3) with added 5% v ethanol. Aqueous electrolyte contained in all cases 0.5 M NaOH.

3. Choice of 1 or 2 Compartment Cells

Figure 1 illustrates 2-compartment cells; however, 1-compartment cells may as well be used both for electricity or hydrogen production. The advantages as well as the limitations in each case are described in the present section. In the case of cells used for production of electricity, removal of the separation membrane will bring the fuel in contact with the counter electrode and the electrocatalyst. This may induce electrocatalytic oxidation of the fuel and create a reverse flow of current, which is translated as a decrease of the V_{oc} of the cell [29,30]. In the same time, removal of the membrane will decrease the internal resistance of the cell and lead to higher current. Thus 1-compartment cells generate higher current but lower voltage than 2-compartment cells [30]. In the case of 2-compartment cells, of course, a chemical bias may also be applied by placing different electrolytes in the two compartments, a property that is absent in 1-compartment cells. Chemical bias will further increase the open-circuit voltage and provide additional drive for cell operation.

In the case of cells used for photoelectrocatalytic hydrogen production, 2-compartment cells provide the possibility to separate hydrogen production from oxidation reactions and thus avoid any loss of hydrogen. In addition, an acidic electrolyte may be introduced in the cathode compartment thus providing a sink of protons that are directly reduced to produce hydrogen [31,32,33]. The separation membrane may then be a proton transfer membrane the functionality of which is preserved in contact with the acidic electrolyte. As shown in Figure 1B, the cathode compartment in that case is sealed while the anode compartment may be exposed to the ambient. An alkaline electrolyte may then be introduced in the photoanode compartment introducing a chemical bias and facilitating fuel oxidation in an alkaline environment [31,33]. Of course, the pH of the electrolyte in the anode compartment may influence the availability of protons and the continuous transfer of protons to the cathode compartment. Therefore, the choice of the electrolytes [32] in the case of chemical bias should be a matter of optimization studies. 2-compartment cells are necessary in the case that water itself is used as a fuel [32,34,35,36] since water oxidation produces oxygen, which must be separated from hydrogen. However, when a fuel is oxidized the oxidation products interfere less with the production of hydrogen. It is then possible to produce hydrogen in a sealed 1-compartment reactor. The whole set up may be very simplified in that case, as in the example of the "photoelectrocatalytic leaf" [5,37] illustrated in Figure 5. The photoelectrocatalytic leaf is one single electrode that carries both a photocatalyst and an electrocatalyst. Photogenerated electrons are directly transferred from the photocatalyst to the electrocatalyst and reduce water producing hydrogen. The advantage of this configuration is the separation of the two catalysts that allows a vast choice of applicable materials and the avoidance of wirings and electrical resistance.

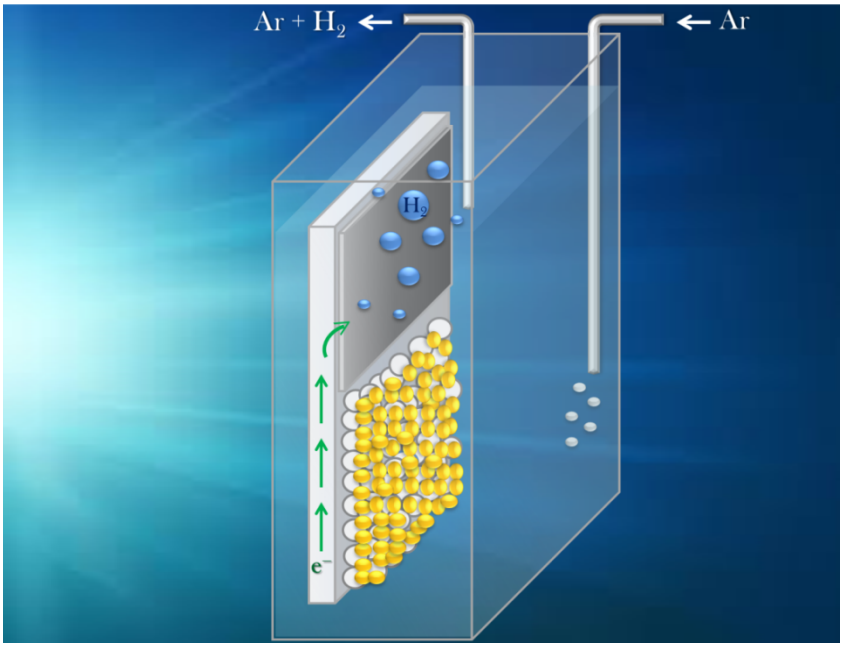

Figure 5. Illustration of a device used for hydrogen production employing a "photoelectrocatalytic leaf" as combined photoanode and cathode electrode. The photocatalyst is a combination of a nanoparticulate oxide semiconductor and a nanoparticulate sensitizer.

4. Choice of Photocatalyst

The photocatalyst used in PFCs is always a mesoporous (nanocrystalline) semiconductor. Mesoporosity is accompanied by a high active surface area that creates a large interface with the electrolyte thus increasing cell functionality. The most popular photocatalyst is the well-known nc-TiO_2. Its popularity stems from the fact that it is efficient, abundant and inexpensive to obtain, easy to manipulate and deposit as thin film, stable and, in principle, not toxic. Titania is used as whitening agent in common commercial paints and titanium itself is among the ten most abundant elements in the earth crust. Titania crystallizes in three different crystalline phases two of which, anatase and rutile, are photocatalytically active. One very popular form of commercial titania, known under the code name P25, consists of about 75% anatase and 25% rutile. This combination makes a very efficient photocatalyst since rutile has a CB lying lower than that of anatase and this allows electron transfer from anatase to rutile that decreases electron-hole recombination probability. The only problem with titania is that it absorbs only UV light, therefore, it must be combined with a sensitizer. A sensitizer may be a dye or another semiconductor with smaller band gap. Dyes or the recently enthusiastically studied organometal halide perovskites [38] are not stable in aqueous electrolytes and they are excluded as sensitizers, unless protected in a tandem cell. In fact, the only applicable sensitizers are a few quantum dots of the II-VI group semiconductors, namely, CdS, ZnSe, CdSe and PbS. Even among these semiconductors, only CdS and ZnSe are applicable with organic fuels, since, as analytically discussed in Section 2 (*cf.* Figure 3), combination of titania with the sensitizer results in a decrease of the combined photocatalyst oxidation level. Thus only CdS/nc-TiO_2 and ZnSe/nc-

TiO_2 combined photocatalysts have been shown to be capable to produce hydroxyl radicals and thus efficiently oxidize organic substances [11,22].

Titania has been deposited in many different nanostructures: nanoparticles, nanorods, nanotubes, nanowires, etc, claiming better electron-hole separation in the case of one-dimensional nanostructures. Our personal experience has, however, led to the conclusion that one-dimensional nanostructures are good if they are perfectly formed and that it is better to use nanoparticulate films, which are easy to form, than risk with poorly formed other type of nanostructures. For this reason, our results are almost exclusively obtained with nanoparticulate titania. Best working photoanodes are made of a two-layer titania, a thin compact bottom layer and a relatively thick top open structure. The bottom layer facilitates the formation of the upper layer, provides a stable film and higher electric contact with the substrate electrode and prevents short circuits. The top layer provides a large interface with the electrolyte. The thickness of the bottom layer may be 100–300 nm while the thickness of the top layer may be up to 10–15 μm. Details on the construction of these films and film images have been published in our presently cited works.

Other researchers have also used ZnO and other metal oxide semiconductors as photocatalysts. They are not better than titania, if all parameters are together taken into account. The only reason to choose some other metal oxide semiconductor is to use a material that absorbs visible light and does not necessitate the presence of a sensitizer, especially, the above toxic metal sulfides and selenides. Several such materials have been studied, among them, the most popular being WO_3, $BiVO_4$ and Fe_2O_3 [32,34,35,36,39]. As seen in Figure 2, all three have a relatively low lying conduction band, therefore, they can only function under strong bias in order to produce hydrogen. In addition, electron-hole recombination in these materials is very extensive and they necessitate a bias anyway to give an appreciable current. Figure 6A presents current-voltage curves for these three photocatalysts in comparison with titania. It is noted that the anodic photocurrent onset appears at different voltages, which are related with the photoanode potential in each case. Indeed, titania, which has the highest lying conduction band also has the lowest anodic photocurrent onset, i.e. the one appearing at the lowest bias. The voltage values on the horizontal axis in Figure 6A are expressed versus RHE (Reversible Hydrogen Electrode) to avoid the interference of the pH in each case, since the data were obtained using different electrolytes at different pH values. Instead, in Figure 6B voltage is depicted as actually measured, i.e. vs Ag/AgCl electrode using the same electrolyte. It is interesting to note that only the cell bearing titania photocatalyst can function without bias, i.e. it can function as PFC producing electricity. When WO_3 or the $BiVO_4$ and Fe_2O_3 (not shown) photoanodes are employed, the cells can function only under bias, therefore, they can be used only for hydrogen production [32,40–44].

Finally, in the search for visible light absorbing photocatalysts, a special reference must be made to the effort of many researchers for band gap engineering by the employment of ternary oxides. In this respect, a recent review [45] gives an excellent account of photocatalysts of perovskite structure.

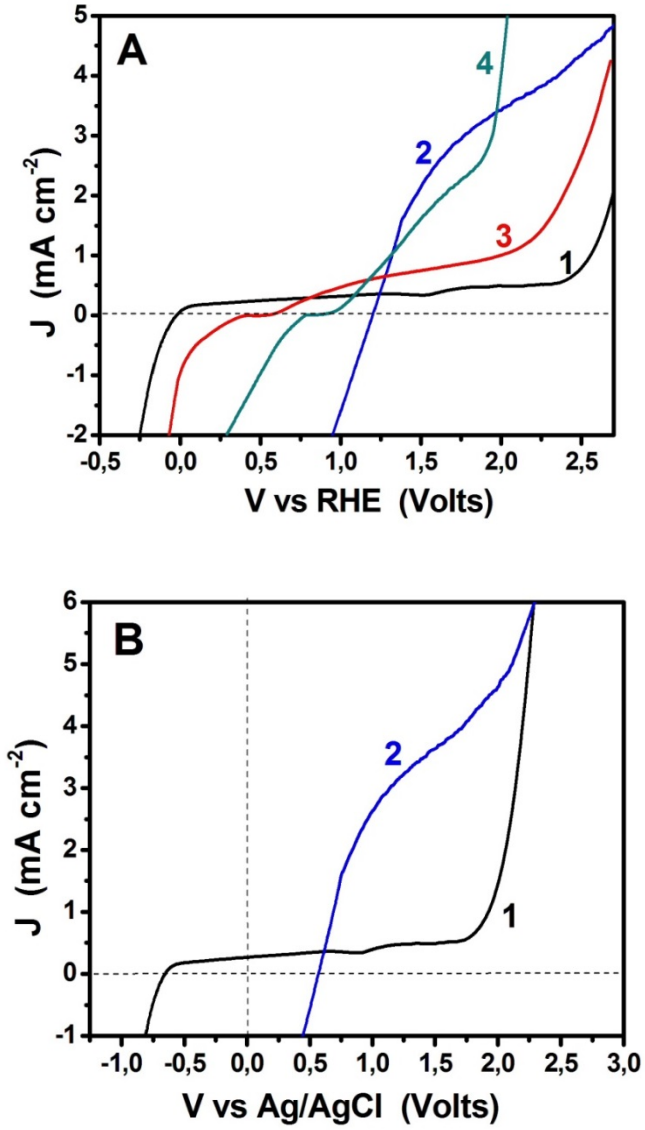

Figure 6. (A) Current-voltage curves for a PFC operating with an aerated cathode and a photoanode carrying various photocatalysts: (1) TiO_2; (2) WO_3; (3) $BiVO_4$ and (4) Fe_2O_3. (B)Similar curves expressed vs Ag/AgCl: (1) TiO_2 and (2) WO_3.

5. Choice of Electrocatalyst

A standard electrocatalyst to be used in PFCs is a blend of carbon black with nanoparticulate Pt. The same electrocatalyst is used on both anode and cathode electrodes in hydrogen fuel cells. This material is very efficient, however, large scale application is discouraged by the rarity and high cost of Pt. In addition, Pt has the tendency to aggregate so that its efficiency progressively decreases. Furthermore, Pt cannot be used with sulfide electrolytes since it interacts with them and it is neutralized. There is intensive research being carried out worldwide to find valuable materials that may efficiently substitute Pt. We are also working in the same domain. The basic properties of an electrocatalyst is that it must be made of a conductive material and must have a large specific surface

area in order to create a large interface with the electrolyte. An interesting material has been described in Ref. [14] and consists of a highly porous sulfur doped carbon nanostructure. It is prepared by doping graphene with a conjugated polymer and by annealing at high temperature. The obtained porous nanostructures were conductive and had a specific surface higher than 600 m^2/g. This functional material was equally efficient as Pt/carbon black electrocatalyst when used as electrocatalyst in PFCs operating in the electricity production mode. More generally, oxygen reduction electrocatalysts, which are being developed for application in Fuel Cells (for example, Ref. [46]) could also be applicable for the operation of PFCs and should be studied for this purpose.

A very simple but also very efficient electrocatalyst was used with sulfide electrolytes [18]. It is simply made by chemical treatment of a brass foil that leads to the formation of a mesoporous Cu_2S layer on brass. Other mesoporous metal sulfide electrocatalysts, such as CuS [47,48] and CoS [47], can be easily grown on electrodes by electrodeposition under ambient conditions. Metal sulfide electrocatalysts are the best choice to use with such type of electrolyte.

6. Choice of Electrode

A standard material used to make photoanode electrodes is Fluorine doped Tin Oxide (FTO), which is transparent and very stable at high temperature annealing. On the contrary, the resistance of Indium-Tin-Oxide (ITO) electrodes increases under heating. Therefore, FTO electrodes is a standard choice for making photoanodes. Of course, if transparency is not an issue, other materials, for example, stainless steel might be applicable.

For cathode electrodes the choice defers for PFCs used for producing electricity from those used for producing hydrogen. In the first case, it is necessary to use a porous electrode that allows oxygen diffusion. For this purpose, the best choice is to use a carbon cloth (*cf.* Ref [11,12,14]). When hydrogen is produced, the electrode can be of any material as long as it provides sufficient active interface with the electrolyte.

7. Choice of Electrolyte

As already discussed, it is preferred that the electrolyte of the anode compartment is alkaline so as to provide an abundant supply of hydroxyl ions. However, some photocatalysts are not stable in alkaline environment, for example WO_3 and $BiVO_4$, where it is necessary to employ a neutral or acidic electrolyte [32,49,50]. In the cathode compartment, it is always preferred to use an acidic electrolyte. In the case of 1-compartment cells, the anode electrolyte is used throughout the cell.

8. Efficiency Issues

The efficiency of PFCs is calculated in the same manner as for any other photoelectrochemical cell [4]. One way to measure cell efficiency is to calculate External Quantum Efficiency (EQE) by means of the Incident Photon to Current conversion Efficiency, IPCE, which is given by the following equation:

$$IPCE = \frac{1240 \times J_{sc}(mA/cm^2)}{\lambda(nm) \times P(mW/cm^2)} \quad (12)$$

where J_{sc} is the short-circuit current density and P the incident radiation intensity at a given wavelength λ. IPCE is a pure number without units. The number 1240 carries the matching units. By recording IPCE at different wavelengths, it is possible to judge the effectiveness of the cell with respect to the spectral response of a photocatalyst or a system of combined photocatalysts or a sensitized catalyst. The value of IPCE is expected to vary between 0 and 1. In most cases IPCE is expressed as IPCE% by multiplying IPCE of Eq. (12) by 100. Thus IPCE% is expected to vary between 0 and 100. Sometimes, IPCE may be found to be larger than 100% due to current doubling phenomena [4,22].

Another way to calculate EQE is given by the following equation [51]:

$$\eta = \frac{\Delta G^0 \times R}{P} \quad (13)$$

where ΔG^0 is the standard Gibbs energy for the photodegradable substance multiplied by the rate R of fuel formation in moles/second and divided by the incident radiation power. If instead of ΔG^0 we use the corresponding potential, calculated by Eq.(6), where n is the number of electrons involved in the photodegradation procedure and F is the Faraday constant, i.e. 96485 C/mol, then

$$\eta = \frac{E \times I}{P} \quad (14)$$

where I is the current involved in the decomposition process. For example, in the case of water splitting E = 1.23 Volts. The value of η, when it refers to hydrogen production by the PFC, will be overestimated if I is taken as the current, which is actually measured with an instrument. The safest way is to calculate I by the value, which corresponds to the quantity of hydrogen produced. Thus if, for example, the device produces 3.5 μmole/min of hydrogen [18], since two electrons correspond to one H_2, we expect that the corresponding current will be I = 2(electrons/molecule) × (3.5×10^{-6} mole/60sec) × 6.023×10^{23} (molecules/mole) × 1.602×10^{-19} (C/electron) = 3.5 μmole/min × 3.22 (mA.min/μmole) = 11.3 mA.

In the case when a bias voltage V_{app} is applied, then Eq. (14) should be substituted by the following equation where the energy supplied to the system is subtracted from the energy produced by the system.

$$\eta = \frac{(E - V_{app}) \times I}{P} \quad (15)$$

When η corresponds to hydrogen production then Eq.(15) gives the so called Solar to Hydrogen efficiency STH. Therefore, for a biased hydrogen production with V_{app}= 0.5 V, for a hydrogen production rate equal to the above 3.5 μmole/min, which corresponds to 11.3 mA, and for an incident radiation of 100 $mWcm^{-2}$, STH (%) = [(1.23 − 0.5) × 11.3/100] × 100% = 8.25%.

9. Conclusions and Perspective

This work has described the basic features of a Photoactivated Fuel Cell (PhotoFuelCell), which can consume an organic or an inorganic fuel to produce electricity or hydrogen. The cell follows the basic configuration of a standard photoelectrochemical cell, it can be easily constructed and it allows a substantial choice of materials both for the construction of the photoanode and the construction of the cathode electrode. Alternative materials for electrocatalyst have been proposed but the matter is open for further research. The experience being obtained by the study of Fuel Cells, where the development of new electrocatalysts is the principle object of research, can offer ideas for the improvement of the operation of PhotoFuelCells and vice versa. Nanoparticulate titania is the uncontested photocatalyst, however, research is open for new visible light absorbing materials. Combination of metals leads to the synthesis of ternary metal oxides, which absorb visible light. Such materials may demonstrate strong potential for application in PhotoFuelCells in parallel with other photocatalytic applications.

Acknowledgements

This project is implemented under the "ARISTEIA" Action of the "OPERATIONAL PROGRAMME EDUCATION AND LIFELONG LEARNING" and is co-funded by the European Social Fund (ESF) and National Resources (Project No.2275).

Conflict of Interest

Authors declare that there is not conflict of interest.

References

1. Becquerel E (1839) Mémoire sur les effets électriques produits sous l'influence des rayons solaires. *Comptes Rendus* 9: 561–567.
2. Fujishima A, Honda K (1972) Electrochemical Photolysis of Water at a Semiconductor Electrode. *Nature* 238: 37–38.
3. Kaneko M, Nemoto J, Ueno H, et al. (2006) Photoelectrochemical Reaction of Biomass and Bio-Related Compounds With Nanoporous TiO_2 Film Photoanode and O_2-Reducing Cathode. *Electrochem Commun* 8: 336–340.
4. Lianos P (2011) Production of Electricity and Hydrogen by Photocatalytic Degradation of Organic Wastes in a Photoelectrochemical Cell: The Concept of the Photofuelcell: A Review of a Re-Emerging Research Field. *J Hazard Mater* 185: 575–590.
5. Michal R, Sfaelou S, Lianos P (2014) Photocatalysis for Renewable Energy Production using PhotoFuelCells. *Molecules* 19: 19732–19750.
6. Shu D, Wu J, Gong Y, et al. (2014) BiOI-based photoactivated fuel cell using refractory organic compounds as substrates to generate electricity. *Catal Today* 224: 13–20.

7. Yang C, He Y, Li K, et al. (2015) Degrading organic pollutants and generating electricity in a dual-chamber rotating-disk photocatalytic fuel cell (RPFC) with a TiO_2 nanotube array anode. *Res Chem Intermed* 41: 5365–5377.
8. Karanasios N, Georgieva J, Valova E, et al. (2015) Photoelectrocatalytic Oxidation of Organics Under Visible Light Illumination: A Short Review. *Curr Org Chem* 19: 512–520.
9. Lu S-J, Ji S-B, Liu J-C, et al. (2015) Photoelectrocatalytic oxidation of glucose at a ruthenium complex modified titanium dioxide electrode promoted by uric acid and ascorbic acid for photoelectrochemical fuel cells. *J Power Sources* 273: 142–148.
10. Li K, Zhang H, Tang T, et al. (2014) Optimization and application of TiO_2/Ti-Pt photo fuel cell (PFC) to effectively generate electricity and degrade organic pollutants simultaneously. *Water Res* 62: 1–10.
11. Sfaelou S, Sygellou L, Dracopoulos V, et al. (2014) Effect of the nature of cadmium salts on the effectiveness of CdS SILAR deposition and its consequences on the performance of sensitized solar cells. *J Phys Chem C* 118: 22873–22880.
12. Antoniadou M, Lianos P (2010) Production of electricity by photoelectrochemical oxidation of ethanol in a PhotoFuelCell. *Appl Catal B* 99: 307–313.
13. Dou B, Song Y, Wang C, et al. (2014) Hydrogen production from catalytic steam reforming of biodiesel byproduct glycerol: Issues and challenges. *Renew Sust Energ Rev* 30: 950–960.
14. Sfaelou S, Zhuang X, Feng X, et al. (2015) Sulfur-doped Porous Carbon Nanosheets as High Performance Electrocatalysts in PhotoFuelCells. *RSC Adv* 5: 27953–27963.
15. Kumagai H, Minegishi T, Sato N, et al. (2015) Efficient solar hydrogen production from neutral electrolytes using surface-modified $Cu(In,Ga)Se_2$ photocathodes. *J Mater Chem A* 3: 8300–8307.
16. Lin C-Y, Mersch D, Jefferson DA, et al. (2014) Cobalt sulphide microtube array as cathode in photoelectrochemical water splitting with photoanodes. *Chem Sci* 5: 4906–4913.
17. Kibsgaard J, Jaramillo TF (2014) Molybdenum Phosphosulfide: An active, acid-stable, earth-abuntant catalyst for the hydrogen evolution reaction. *Angew Chem Int Ed* 53: 14433–14437.
18. Antoniadou M, Sfaelou S, Dracopoulos V, et al. (2014) Platinum-free photoelectrochemical water splitting. *Catal Commun* 43: 72–74.
19. Buhler N, Meier K, Reber J-F (1984) Photochemical Hydrogen Production with Cadmium Sulfide Suspensions. *J Phys Chem* 88: 3261–3268.
20. Daskalaki VM, Panagiotopoulou P, Kondarides DI (2011) Production of peroxide species in Pt/TiO_2 suspensions under conditions of photocatalytic water splitting and glycerol photoreforming. *Chem Eng J* 170: 433–439.
21. Sakata T, Kawai T (1981) Heterogeneous photocatalytic production of hydrogen and methane from ethanol and water. *Chem Phys Lett* 80: 341–344.
22. Antoniadou M, Kondarides DI, Dionysiou DD, et al. (2012) Quantum dot sensitized titania applicable as photoanode in photoactivated fuel cells. *J Phys Chem* 116: 16901–16909.
23. Kondarides DI, Daskalaki VM, Patsoura A, et al. (2008) Hydrogen production by photo-induced reforming of biomass components and derivatives at ambient conditions. *Catal Lett* 122: 26–32.
24. Rossetti I (2012) Review article: Hydrogen production by photoreforming of renewable substrates. *ISRN Chem Eng* 2012 Article ID 964936: 21 pages, doi:10.5402/2012/964936.

25. Panagiotopoulou P, Antoniadou M, Kondarides DI, et al. (2010) Aldol Condensation Products During Photocatalytic Oxidation of Ethanol in a Photoelectrochemical Cell. *Appl Catal B* 100: 124–132.
26. Antoniadou M, Panagiotopoulou P, Kondarides DI, et al. (2012) Photocatalysis and Photoelectrocatalysis Using Nanocrystalline Titania Alone or Combined with Pt, RuO_2 or NiO Co-Catalysts. *J Appl Electrochem* 42: 737–743.
27. Maeda Y, Fujishima A, Honda K (1981) The Investigation of Current Doubling Reactions on Semiconductor Photoelectrodes by Temperature Change Measurements. *J Electrochem Soc* 178: 1731–1734.
28. Kalamaras E, Lianos P (2015) Current doubling effect revisited: Current multiplication in a PhotoFuelCell. *J Electroanal Chem* 751: 37–42.
29. Antoniadou M, Han C, Sfaelou S, et al. (2013) Solar energy conversion using Photo-Fuel-Cells. *Sci Adv Mater* 5: 1–8.
30. Antoniadou M, Sfaelou S, Lianos P (2014) Quantum dot sensitized titania for photo-fuel-cell and for water splitting operation in the presence of sacrificial agents. *Chem Eng J* 254: 245–251.
31. Antoniadou M, Lianos P (2009) Near Ultraviolet and Visible light photoelectrochemical degradation of organic substances producing electricity and hydrogen. *J Photochem Photobiol A* 204: 69–74.
32. Monfort O, Pop L-C, Sfaelou S, et al. (2016) Photoelectrocatalytic hydrogen production by water splitting using $BiVO_4$ photoanodes. *Chem Eng J* 286: 91–97.
33. Selli E, Chiarello GL, Quartarone E, et al. (2007) A photocatalytic water splitting device for separate hydrogen and oxygen evolution. *Chem Commun* 5022–5024.
34. Gan J, Lu X, Tong Y (2014) Towards highly efficient photoanodes: boosting sunlight-driven semiconductor nanomaterials for water oxidation. *Nanoscale* 6: 7142–7164.
35. Horiuchi Y, Toyao T, Takeuchi M, et al. (2013) Recent advances in visible-light-responsive photocatalysts for hydrogen production and solar energy conversion-from semiconducting TiO_2 to MOF/PCP photocatalysts. *Phys Chem Chem Phys* 15: 13243–13253.
36. Bhatt MD, Lee JS (2015) Recent theoretical progress in the development of photoanode materials for solar water splitting photoelectrochemical cells. *J Mater Chem A* 3: 10632–10659.
37. Pop LC, Dracopoulos V, Lianos P (2015) Photoelectrocatalytic hydrogen production using nanoparticulate titania and a novel Pt/Carbon electrocatalyst: The concept of the "Photoelectrocatalytic Leaf". *Appl Surf Sci* 333: 147–151.
38. Gao P, Grätzel M, Nazeeruddin MK (2014) Organohalide lead perovskites for photovoltaic applications. *Energy Environ Sci* 7: 2448–2463.
39. Alexander BD, Kulesza PJ, Solarska R, et al. (2008) Metal Oxide photoanodes for solar hydrogen production. *J Mater Chem* 18: 2298–2303.
40. Fujimoto I, Wang N, Saito R, et al. (2014) $WO_3/BiVO_4$ composite photoelectrode prepared by improved auto-combustion method for highly efficient water splitting. *Int J Hydrogen Energ* 39: 2454–2461.
41. Zhu T, Chong MN, Chan ES (2014) Nanostructured Tungsten Trioxide Thin Films Synthesized For Photoelectrocatalytic Water Oxidation: A Review. *Chem Sus Chem* 7: 2974–2997.

42. Liu X, Wang F, Wang Q (2012) Nanostructure-Based WO_3 Photoanodes For Photoelectrochemical Water Splitting. *Phys Chem Chem Phys* 14: 7894–7911.
43. Mirbagheri N, Wang D, Peng C, et al. (2014) Visible Light Driven Photoelectrochemical Water Oxidation by Zn- and Ti-Doped Hematite Nanostructures. *ACS Catal* 4: 2006–2015.
44. Mishra M, Chun D-M (2015) α-Fe2O3 as a photocatalytic material: A review. *Appl Catal A* 498: 126–141.
45. Wang W, Tade MO, Shao Z (2015) Research progress of perovskite materials in photocatalysis- and photovoltaics-related energy conversion and environmental treatment. *Chem Soc Rev* 44: 5371–5408.
46. Brüller S, Liang H-W, Kramm UI, et al. (2015) Bimetallic porous porphyrin polymer-derived non-precious metal electrocatalysts for oxygen reduction reactions. *J Mater Chem* 3: 23799–23808.
47. Xi FX, Liu HC, Li WP, et al. (2015) Fabricating CuS counter electrode for quantum dots-sensitized solar cell via electro-deposition and sulfurization of Cu_2O. *Electrochim Acta* 178: 329–335.
48. Balis N, Dracopoulos V, Bourikas K, et al. (2013) Quantum dot sensitized solar cells based on an optimized combination of ZnS, CdS and CdSewith CoS and CuS counter electrodes. *Electrochim Acta* 91: 246–252.
49. Sayama K, Nomura A, Zou Z, et al. (2003) Photoelectrochemical decomposition of water on Nanocrystalline $BiVO_4$ film electrodes under visible light. *Chem Commun* 2908–2909.
50. Liu X, Wang F, Wang Q (2012) Nanostructure-Based WO_3 Photoanodes For Photoelectrochemical Water Splitting. *Phys Chem Chem Phys* 14: 7894–7911.
51. Varghese OK, Grimes CA (2008) Appropriate strategies for determining the photoconversion efficiency of water photoelectrolysis cells: A review with examples using Titania nanotube array photoanodes. *Sol Energy Mater Sol Cells* 92: 374–384.

AIMS Press